ACS APPLIED MATERIALS & INTERFACES

Letter

www.acsami.org

Piezospectroscopic Measurements Capturing the Evolution of Plasma Spray-Coating Stresses with Substrate Loads

Gregory Freihofer,[†] Daniela Fugon-Dessources,[†] Emrecan Ergin,[‡] Amy Van Newkirk,[¶] Ankur Gupta,[§] Sudipta Seal,[§,∥] Axel Schülzgen,[¶] and Seetha Raghavan*,[†]

[†]Mechanical and Aerospace Engineering Department, [¶]CREOL, The College of Optics and Photonics, [§]Advanced Materials Processing Analysis Center (AMPAC) and Nanoscience Technology Center, [∥]Materials Science and Engineering and College of Medicine, University of Central Florida, Orlando, Florida, United States

[‡]Advanced Engineering Materials, Chalmers University of Technology, Gothenburg, Sweden

ABSTRACT: Plasma-spray coatings have a unique microstructure composed of various types of microcracks and weakly bonded interfaces which dictate their nonlinear mechanical properties. The intrinsic photo-luminescence (PL) characteristics of alpha-alumina (α-Al_2O_3) within these coatings offer a diagnostic functionality, enabling these properties to be probed experimentally at the microscale, under substrate loading. The piezospectroscopic (PS) measurements from the coatings are capable of revealing microstructural stress at high spatial resolution. Here, for the first time, the evolution of stresses within air plasma spray (APS) coatings under increasing substrate loads were captured using piezospectroscopy. With mechanical cycling of the substrate, the PS properties revealed anelastic and inelastic behavior and a relaxation of residual tensile stress within the APS coatings. With decreasing substrate thickness, the coating was observed to sustain more stress, as the substrate's influence on the mechanical behavior decreased. The findings provide an insight into the microstructural response that can serve as the basis for model validation and subsequently drive the design process for these coatings.

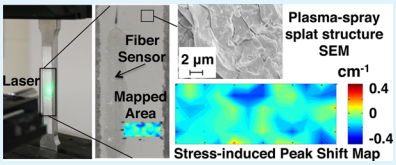

KEYWORDS: *piezospectroscopy, plasma-spray, coating, stress, mechanical testing, photo-luminescence*

INTRODUCTION

Plasma-spray coatings have been commonly used in the fields of corrosion and wear resistance and as thermal barrier coatings for thermal protection.[1] The performance of these coatings is heavily dependent on the complex microstructure that results from the thermal spraying process.[2,3] The state of stress and evolution thereof is important because of its influence on the functional properties of the coating.[4]

Macroscale stresses in plasma-sprayed coatings are characterized with a variety of methods including strain gauges[5−7] and laser displacement sensors[7,8] for mechanical and thermal testing respectively. High-resolution microstructural strain measurements for these coatings are available with neutron scattering,[9,10] or synchrotron X-ray diffraction (XRD).[10,11] Piezospectroscopy is a technique that provides multiscale spatial resolution with the benefit of accessibility, while limited to surface and micro-scale depth penetration. Development of the instrumentation for measurements described in this work requires integration of spectroscopy, spatial mapping and loading systems for in situ mechanical testing.[12]

PS can be used for a variety of materials that possess stress-sensitive photoluminescence or Raman emissions.[13] This work focuses on the prominent and highly investigated spectral emission peaks of α-Al_2O_3 known as the R-lines. These emissions are the result of laser excitation of the material and have been used for sensing pressure in diamond anvil cells.[14,15] In thermally grown oxides of thermal barrier coatings, the signature R-line peaks R1 and R2 offer a method to quantify the stresses in this layer[16] and the corresponding life of the coating. More recently, PS properties have been used in a variety of ways including the verification of stresses with finite element models,[17] the study of fracture mechanisms in advanced ceramics[13] and the development of stress-sensing nanomaterials.[18] This work aims to use the spectral peaks from α-Al_2O_3 in plasma-spray coatings to probe the microstructural stresses in the coating directly while the substrate is subjected to tensile loads. Effects of the variation of substrate thickness as well as the effect of cyclic loading on the coating stress are investigated.

EXPERIMENTAL PROCEDURE

In this study, the pure feedstock contained 95 and 5% α and γ-Al_2O_3 respectively. Phase transformation occurred during processing and XRD results in Figure 2a established that the final content was 75% γ- and 25% α-phase. The 200-300μm thick coating was applied to aluminum 2024 dogbone-shaped specimens manufactured according to ASTM E8-04 standard[19] with 1/8, 1/5, and 1/4 in. substrate thicknesses. The tensile cyclic loading conditions shown in Figure 1c were scaled with respect to the yield stress of aluminum and stress amplitudes progressively increased to 15, 30, and 60% yield. The 1/5 in. substrate was precycled twice to 60% yield before the cyclic conditions in Figure 1c were applied to investigate the effects of additional loading and unloading. The steps in the loading cycle represent the force control hold for 5 minutes allowing the probe to collect the spectral maps highlighted in Figure 1b. A fiber Bragg grating (FBG) sensor, shown in Figure 1b, was attached directly to the

Received: November 6, 2013
Accepted: January 14, 2014
Published: January 14, 2014

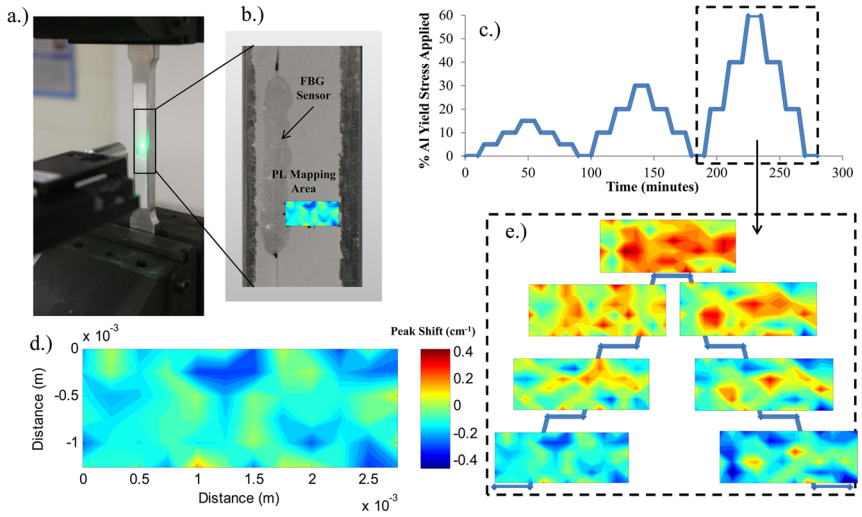

Figure 1. (a) Coupled load frame and spectrometer probe setup, (b) view of the gauge section, (c) the tensile load cycle, (d) peak shift distribution map before the 3rd cycle begins, and (e) a highlighted section of the load cycle with corresponding peak shift distribution maps.

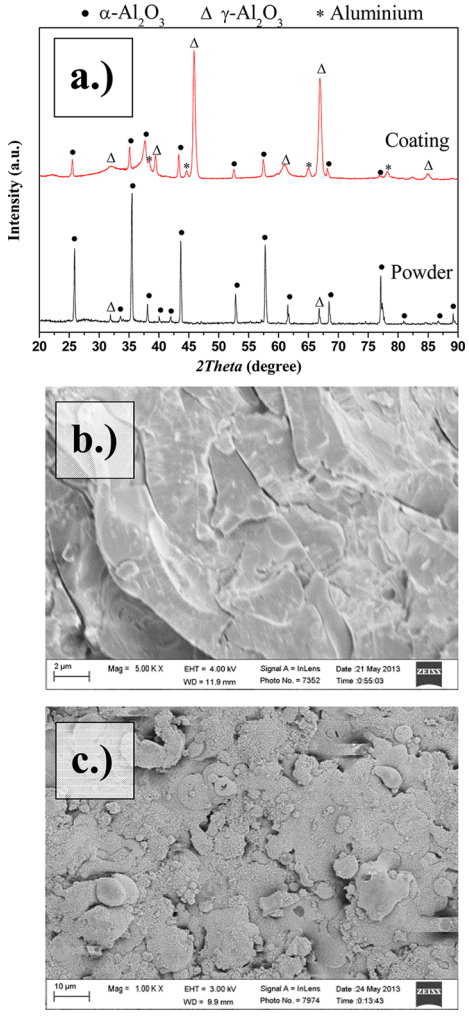

Figure 2. (a) XRD of the Al_2O_3 powder and coating and (b, c) SEM images of the APS Al_2O_3 coating on the 1/5 in. substrate with a (b) cross-sectional and (c) top surface view.

plasma coating to verify good adhesion between the coating and the substrate.

The hyperspectral data was obtained using a unique experimental setup[12] consisting of an integrated spectrometer, XYZ-stage, and a mechanical load frame shown in Figure 1a. The maps were collected in a 12 × 6 snake scan pattern over a 3 × 1.5 mm area outlined in Fig. 1b. These peak shift maps (Fig. 1d) were recorded for every mechanical force controlled hold (Figure 1e). The spectral map edges were truncated to remove any effect of variable coating thickness on the right edge or the presence of the adhesive from the FBG on the left edge. The PS peak shift data were obtained from deconvolution of the R-lines[20] as an average of 56 data points with reference to their local zero load peak position.

RESULTS AND DISCUSSION

The average difference between stress measured by the FBG sensor and the stress applied was approximately 6% throughout all mechanical cycles. This small difference between the applied mechanical stress and the stress measured by the FBG fiber is depicted in Figure 3a and validates that the coating remained adhered to the substrate for the duration of the test.

The microstructure of the APS coating must be considered when one interprets Fig. 3b. The extremely rapid cooling of molten splats from the APS process creates a layered splat microstructure with complex geometry.[21] This creates partial bonding between the lamellar structure and when combined with the brittle nature of the pure Al_2O_3 coating, it produces inelastic[6,7] and anelastic[22] mechanical behavior.

Anelastic behavior is defined as nonlinear, reversible deformation while inelastic behavior is represented by irreversible deformation. Both of these intrinsic mechanical characteristics to APS coatings were seen to be carried into the PS properties. The inelastic behavior was more evident in PS data (Figure 3b) as compared to the FBG data (Figure 3a) highlighting the ability to probe the micromechanics more directly with the piezospectroscopic measurements. Upon releasing the mechanical load, the PS measurements indicate the coating was releasing strain energy because of the relative downshift in peak position when returning to zero load. This could be a sign of relaxation of the coating's tensile "quenching stress" from rapid cooling of the molten ceramic during the APS process.[10,11,23] This relaxation is likely to occur from the breaking of weak bonds from the extremely brittle nature of Al_2O_3, sliding of splat interfaces during mechanical loading, or opening and closing of microcracks.

Non recoverable deformation occurred for all three substrates. However, the sample that was pre-cycled twice to 60% yield

dx.doi.org/10.1021/am404985k | ACS Appl. Mater. Interfaces 2014, 6, 1366−1369

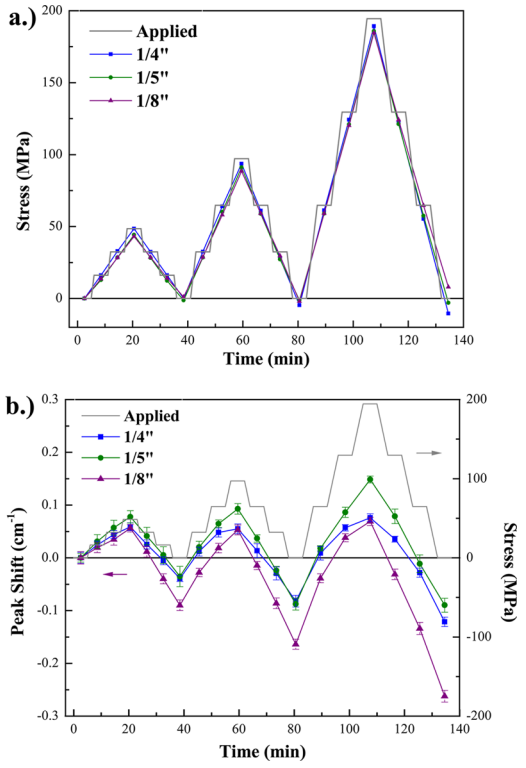

Figure 3. FBG sensor stress (a) on the coating surface and (b) the PL peak shift for R1 for all three substrate thicknesses. The error bars represent one standard deviation of the peak shift in the mapped area.

showed recoverable deformation in Figure 4c when the inelastic behavior became anelastic with continued mechanical cycling. The two other substrate thicknesses of 1/8 and 1/4 in. have similar inelastic behavior with some recoverable response until new stress amplitudes were reached. With increasing stress amplitudes, the PS nonlinearity increases.

PS properties are normally defined by just a first order PS coefficient. Preferably R2 is used for stress measurements because it behaves linearly with stress.[16] However, for the APS coating studied here R1 and R2 were both nonlinear and this is likely due to the evolving mechanical properties from damage induced to the coating during mechanical loading. For the lower stress amplitude cycles there was a first-order relationship, but for larger amplitude cycles a higher-order relationship was observed. Normally, higher order PS coefficients only arise in the presence of extremely large stresses.[15] However, the APS coating's microstructural features provide a variety of stress concentrations in the form of horizontal and vertical microcracks.[23] Nonlinearities in macroscale measurements for APS coatings have been attributed to a combination of unique geometrical/microstructural features[7] as seen in Figure 2. Even for the brittle Al_2O_3, there is expected to be some finite amount of plastic deformation occurring during crack propagation,[24] and could contribute to this nonlinear mechanical behavior which has been called "pseudoplastic".[8]

Figure 4d shows the first-order PS coefficient decreasing with subsequent cycles and increasing stress amplitudes. Additionally, the PS coefficients are significantly different for loading and unloading. Consistently, the PS coefficients are larger for unloading. A stiffening behavior during unloading attributed to microcrack interfaces sticking to each other upon load reversal has been modeled in literature.[22] Also, it has been established that Young's modulus increases under compression for APS coatings because of the reduced density of microcracks from crack closures.[23] The variation in PS coefficient serves as a representation of this microstructural behavior.

Competing effects that control the PS coefficient were observed. Upon release of the mechanical load, the coating relaxes and gradually approaches a compressive state leading to an increased stiffness for APS coatings.[22,23] This increases the PS coefficient as observed between the differences for loading and unloading in Figure 4d. However, the brittle nature of the Al_2O_3 microstructure makes it susceptible to various forms of microstructural damage upon mechanical loading,[23] which would decrease the PS coefficient. Overall, the additional damage with increasing stress amplitude appears to be overcoming the stiffening effect from a more compressive state. However, a constant stress amplitude fatigue study may be necessary to understand the convergence in the PS coefficient with multiple cycles. The possibility of convergence is supported by the PS response of the 1/5 in. substrate in Figure 4c. This substrate thickness, preloaded twice to 60% yield, had a convergent PS coefficient for loading and unloading in the last cycle.

Substrate thickness had substantial effects on the PS coefficient observed in Fig. 4d, where thinner substrates resulted in higher PS coefficients. An increasing ratio of coating to substrate thickness causes the plasma spray coating to sustain more stress as the substrates influence on the mechanical response diminishes.

The coating's micromechanics were observed with mechanical cycling of the substrate *via* PS measurements, demonstrating the capability for observing the Al_2O_3 microstructural behavior. The addition of reinforcing materials into the APS

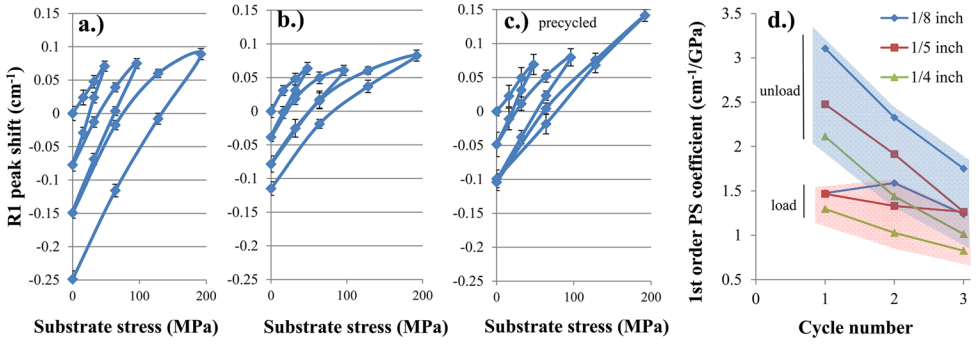

Figure 4. Cyclic response of the peak shift with respect to substrate stress for the (a) 1/8 in., (b) 1/4 in., and (c) the precycled 1/5 in. substrate. (d) The first-order PS coefficients for each substrate thickness as a function of cycle number. The error bars represent one standard deviation of the peak shift in the mapped area.

dx.doi.org/10.1021/am404985k | ACS Appl. Mater. Interfaces 2014, 6, 1366−1369

feedstock such as Aluminum particles[25] or Carbon nanotubes[26−28] has been shown to increase fracture toughness, prolong fatigue life and decrease the nonlinear behavior.[23] PS could be used to assess, through microstructural studies, the mechanical improvement from these reinforcements.

CONCLUSION

In conclusion, the plasma-spray Al_2O_3 coating showed distinct PS properties indicative of the complex microstructural changes under substrate load. The ability to observe the micromechanics of coating deformation under mechanical cycling of the substrate with micrometer-level spatial resolution makes the PS measurements advantageous for coating studies. Here, it was shown how piezospectroscopic data serve as micromechanical measurements that can supplement the design of plasma spray coatings. Future work will target higher spatial resolutions, cyclic fatigue tests, and SEM studies correlating microcrack density with the convergence or variation of the PS coefficient.

AUTHOR INFORMATION

Corresponding Author

*E-mail: seetha.raghavan@ucf.edu.

Notes

The authors declare no competing financial interest.

ACKNOWLEDGMENTS

This material is based on work supported by the National Science Foundation under Grant CMMI 1130837 and the University of Central Florida Office of Research and Commercialization Inhouse Grant FY 2012. Plasma Spray Laboratory was funded through a ONR DURIP grant and YIP award to S.S. Ms. Hong Tat from Boeing Research & Technology is acknowledged for technical discussions.

REFERENCES

(1) Crawmer, D. *Encyclopedia of Materials: Science and Technology*,- second ed.; Elsevier: Oxford, U.K., 2001; pp 7035−7040.
(2) Hawthorne, H.; Erickson, L.; Ross, D.; Tai, H.; Troczynski, T. *Wear* **1997**, *203-204*, 709−714.
(3) Agarwal, A.; McKechnie, T.; Seal, S. *J. Therm. Spray Technol.* **2003**, *12*, 350−359.
(4) Freund, L.; Suresh, S. *Thin Film Materials: Stress, Defect Formation, and Surface Evolution*; Cambridge University Press: Cambridge, U.K., 2003.
(5) Harok, V.; Neufuss, K. *J. Therm. Spray Technol.* **2001**, *10*, 126−132.
(6) Rejda, E. F.; Socie, D. F.; Itoh, T. *Surf. Coat. Technol.* **1999**, *113*, 218−226.
(7) Dwivedi, G.; Nakamura, T.; Sampath, S. *J. Am. Ceram. Soc.* **2011**, *94*, S104−S111.
(8) Musalek, R.; Matejicek, J.; Vilemova, M.; Kovarik, O. *J. Therm. Spray Technol.* **2010**, *19*, 422−428.
(9) Allen, A. J.; Ilavsky, J.; Long, G. G.; Wallace, J. S.; Berndt, C. C.; Herman, H. *Acta Mater.* **2001**, *49*, 1661−1675.
(10) Kesler, O.; Matejicek, J.; Sampath, S.; Suresh, S.; Gnaeupel-Herold, T.; Brand, P. C.; Prask, H. J. *Mater. Sci. Eng., A* **1998**, *A257*, 215−224.
(11) Kovářík, O.; Siegl, J.; Nohava, J.; Chráska, P. *J. Therm. Spray Technol.* **2005**, *14*, 231.
(12) Freihofer, G.; Poliah, L.; Walker, K.; Medina, A.; Raghavan, S. *J. Instrum.* **2010**, *5*, P12003.
(13) Pezzotti, G. *J. Raman Spectrosc.* **1999**, *30*, 867−875.
(14) Piermarini, G. J.; Block, S.; Barnett, J. D.; Forman, R. A. *J. Appl. Phys.* **1975**, *46*, 2774.
(15) Eggert, J. H.; Goettel, K. A.; Silvera, I. F. *Phys. Rev. B* **1989**, *40*, 5742.
(16) Selcuk, A.; Atkinson, A. *Mater. Sci. Eng., A* **2002**, *A335*, 147−156.
(17) Porporati, A. A.; Miyatake, T.; Schilcher, K.; Zhu, W.; Pezzotti, G. *J. Eur. Ceram. Soc.* **2011**, *31*, 2031−2036.
(18) Stevenson, A.; Jones, A.; Raghavan, S. *Nano Lett.* **2011**, *11*, 3274.
(19) *ASTM Standard Test Methods for Tension Testing of Metallic Materials*; ASTM International: West Conshohocken, NJ, 2008.
(20) Raghavan, S.; Imbrie, P. *Appl. Spectrosc.* **2008**, *62*, 759−765.
(21) Li, C.-J.; Ohmori, A. *J. Therm. Spray Technol.* **2002**, *11*, 365−374.
(22) Liu, Y.; Nakamura, T. *J. Am. Ceram. Soc.* **2008**, *91*, 4036−4043.
(23) Kroupa, F. *J. Therm. Spray Technol.* **2007**, *16*, 84.
(24) Balic, E. E.; Hadad, M.; Bandyopadhyay, P. P.; Michler, J. *Acta Mater.* **2009**, *57*, 5921−5926.
(25) Yin, Z.; Tao, S.; Zhou, X.; Ding, C. *Appl. Surf. Sci.* **2008**, *254*, 1636−1643.
(26) Balani, K.; Agarwal, A. *J. Appl. Phys.* **2008**, *104*, 063517.
(27) Balani, K.; Zhang, T.; Karakoti, A.; Li, W.; Seal, S.; Agarwal, A. *Acta Mater.* **2008**, *56*, 571−579.
(28) Zou, J.; Liu, J.; Karakoti, A. S.; Kumar, A.; Joung, D.; Li, Q.; Khondaker, S. I.; Seal, S.; Zhai, L. *ACS Nano* **2010**, *4*, 7293−7302.